Sequence and Dispersity are Determinants of Photodynamic Antibacterial Activity Exerted by Peptidomimetic Oligo(thiophene)s

Zhe Zhou, ¹ Cansu Ergene, ¹ Joshua Y. Lee, ² David J. Shirley, ² Benjamin R. Carone, ³ Gregory A. Caputo^{2,3} and Edmund F. Palermo^{1,*}

¹Rensselaer Polytechnic Institute, Materials Science and Engineering, Troy, NY 12054
²Rowan University, Department of Chemistry and Biochemistry, Glassboro, NJ 08028
³Rowan University, Department of Molecular & Cellular Biosciences, Glassboro, NJ 08028

*Email: palere@rpi.edu

Keywords: Antibacterial, Photodynamic, Sequence, Biomimetic, Cytotoxicity, Drug discovery

Abstract

A library of functionalized oligo(thiophene)s with precisely controlled chain length, regioregularity, sequence, and pendant moieties in the side chains, was prepared by iterative convergent/divergent organometallic couplings. The cationic and facially amphiphilic structures were designed to mimic the salient physiochemical features of host defense peptides (HDPs) while concurrently exerting a photodynamic mechanism of antibacterial activity. In the dark, the oligothiophenes exert broad-spectrum and rapid bactericidal activity in the micromolar regime, which is the typical range of HDP activity. Under visible light, the antibacterial potency is enhanced by orders of magnitude, leading to potency in the nanomolar concentration range, whereas the toxicity to red blood cells is almost unaffected by the same visible light exposure. We attribute the potent and selective antibacterial activity to a dual mechanism of action that involves bacterial cell binding, combined with ROS production in the bound state. Comonomer sequence and chain length dispersity play important roles in dictating the observed biological activities. The most promising candidate compound from a set of screening experiments showed antibacterial activity that is three orders of magnitude more potent against bacteria relative to toxicity against RBCs. Importantly, this compound did not induce resistance upon 21 subinhibitory passages, whereas the activity of Ciprofloxacin was reduced 32× in the same condition. Cytotoxicity against HeLa cells in vitro is orders of magnitude weaker than antibacterial activity under visible light illumination. Thus, we have established a new class of HDP-mimetic antibacterial compounds with nanomolar activity and cell type selectivity of greater than 1300-fold. These and related compounds may be highly promising candidates in the urgent search for new topical photodynamic antibacterial formulations.

Introduction

The alarmingly rapid proliferation of antibiotic drug-resistant bacterial infections, exacerbated by the shrinking arsenal of new antibiotic drug approvals, has created a looming public health crisis. Host defense peptides (HDPs)²⁻⁵ and their synthetic polymer mimics⁶⁻⁹ show promise as broad-spectrum antibiotics that do not induce resistance, 10 by a putative mechanism involving membrane disruption. 11-12 Although the native peptide sequences suffer from proteolytic instability and poor pharmacokinetics, 13 synthetic mimics of HDPs have recently advanced to clinical trials. 14-15 Photodynamic therapy is a highly promising route to next-generation antibiotics that are activated by light to generate reactive oxygen species (ROS) that are toxic to microbes. 16 Whitten and co-workers pioneered water-soluble π -conjugated polyelectrolytes with pendant quaternary ammonium salt (QAS) groups as light-activated antibacterial agents, starting in 2005. The Since then, many research groups have designed and synthesized π -conjugated polymers¹⁸⁻²⁵ and oligomers²⁶⁻²⁹ that contain pendant cationic moieties (typically QAS or imidazole) to mediate bacterial inactivation via photodynamic effects.³⁰ Interestingly, one study revealed that tertiary amines were more effective antibacterial agents as directly compared to QAS analogues, suggesting that the chemical structure of the cationic groups is a key determinant of photodynamic activity.³¹

Whereas structure-activity relationship (SAR) studies among HDPs and their synthetic polymer mimics have been reported extensively in the past few decades, $^{32-35}$ there is still a relative paucity of precisely detailed SAR data regarding photodynamic cationic π -conjugated systems, especially with regards to HDP-mimetic analogues. Thus, we sought to converge HDP-mimetic molecular design principles into the context of photodynamic activity, using sequence controlled π -conjugated oligomers of thiophene as an example platform (Figure 1). Encouraged

by literature precedent on "facially amphiphilic" antimicrobial arylamide oligomers³⁶⁻³⁹ and photodynamic π -conjugated polymers/oligomers,^{20, 40-42} we endeavored to design thiophene oligomers with HDP-mimetic structures that absorb visible light, thus producing ROS on demand. In particular, we targeted oligo(thiophene) derivatives via convergent/divergent iterative Stille coupling,⁴³ which yields precisely controlled unimolecular chain length, regionegularity, and comonomer sequence.⁴⁴ The target comonomers are the hydrophobic 3-methyl thiophene and 3-(2-aminoethyl)thiophene, which is cationic by virtue of protonation in aqueous buffers of neutral pH. Alternating copolymers of these two repeat units are expected to prefer conformations that project the cationic groups to one face of the molecule while projecting the hydrophobic groups to the opposite face. This "facially amphiphilic" segregation of

hydrophobic and cationic character is a hallmark of HDP-mimetic design. 45-47

The photodynamic antibacterial polymers reported to date contain charged permanently quaternary ammonium salt (QAS) or imidazolium groups, as the source of cationic charge, whereas **HDPs** employ reversibly protonated primary amine groups (Lys) (Arg).⁴⁸ and/or guanidine Primary

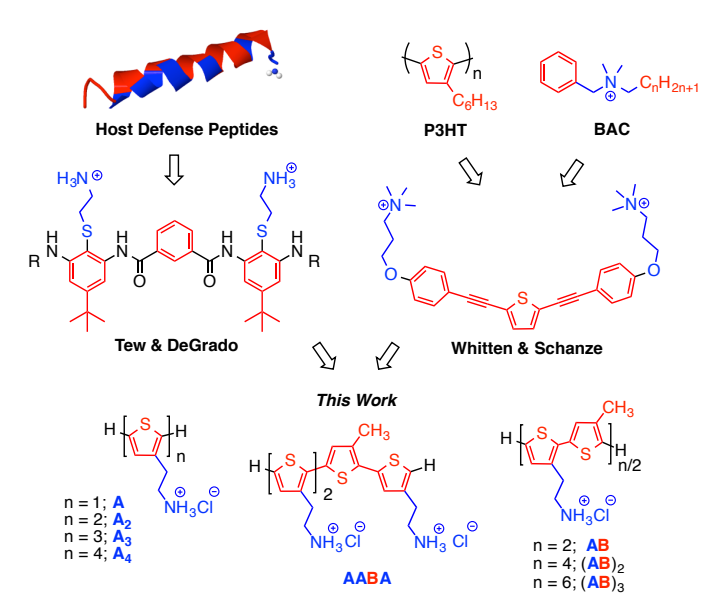


Figure 1. Convergence of molecular design principles from HDP-mimetic antibacterials and photodynamic π -conjugated oligomers. Primary amines are intended to mimic the lysine residues that are abundant in HDPs.

amines that are cationic by virtue of protonation (-NH₃⁺) differ in subtle but important ways from permanently charged QAS groups (*e.g.* -N(CH₃)₃⁺) in terms of antibacterial potency.⁴⁹ Indeed, prior studies on HDP-mimetic polymers have shown that protonated primary amines

outperform their QAS counterparts, in a direct comparison.⁵⁰⁻⁵¹ These results are understood in terms of the binding affinity between protonated primary amines and the anionic phospholipid head groups present in the bacterial cell membrane, which are enhanced by hydrogen bonding interactions not accessible to the QAS groups.⁵² Accordingly, we designed sequence-controlled and monodisperse oligo(thiophene)s with *primary* amine groups pendant in the side chains, as source of reversibly protonated cationic charge (¬NH₃⁺). We employed the synthetic strategy of iterative convergent/divergent coupling of oligothiophenes⁴³ bearing functional groups in the side chains for further modification.⁴⁴ The resulting compounds are soluble in aqueous buffers and bear a cationic charge at neutral pH. The hydrophobicity of the thiophene backbone renders the structure "facially amphiphilic" at the repeat unit level. Control of comonomer sequence, unimolecular chain length, and dispersity (or lack thereof) are accessible by this methodology.

Results and Discussion

Oligomer Synthesis. Alternating oligomers of 3-thiophene ethanol and 3-methyl thiophene were prepared convergent/divergent iterative coupling⁴³⁻⁴⁴ (Figure 2). Detailed synthetic procedures are given in the SI. Briefly, thiophene ethanol was first protected as a silyl ether, bromination was carried out with Nbromosuccinimide (NBS), and stannylation was performed with lithium diisopropyl amide (LDA) and tributyl tin chloride at low temperature

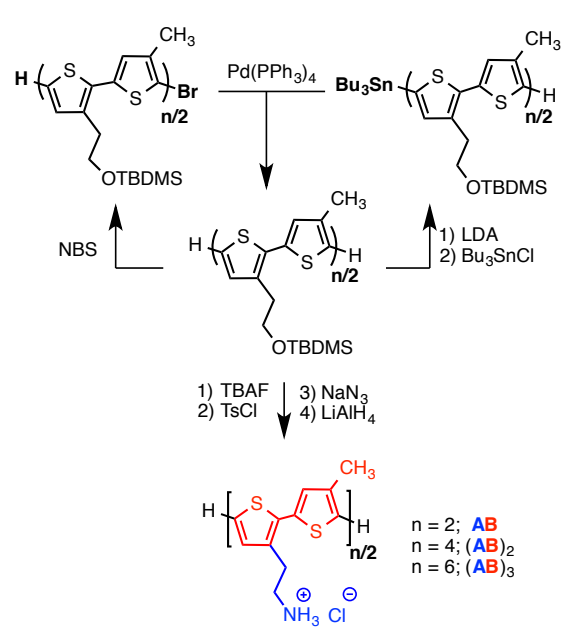


Figure 2. Iterative convergent/divergent synthesis of precise unimolecular oligomers of thiophene bearing cationic and hydrophobic side chains.

(-78 °C). Stille coupling was performed at 90 °C in toluene with 1 mol% Pd(PPh₃)₄ catalyst. After coupling, the *tert*-butyldimethylsilane (TBDMS) protected alcohol groups were converted to amines via reduction of the azide intermediate. The unimolecular nature of the oligomers was confirmed by matrix-assisted laser desorption ionization (MALDI) time-of-flight mass spectroscopy, and their regioregularity was quantified by 1 H NMR. In addition to the alternating sequences, named [AB]_{n/2} (n = 2, 4, 6), we also prepared homooligomers in which every repeat unit bears an amino group, dubbed [A]_n (n = 1, 2, 3, 4), as well as several other sequences such as the block-like AABB and BAAB, as well as other compositions including AAB and AABA, for example (Table 1).

Table 1. Antibacterial and Hemolytic Activities in the Light and Dark.

Compound	n*	$f_{ m methyl}^{\#}$	MW (g/mol)	MIC ⁺ (μg/mL)		HC ₅₀ (μg/mL)		HC ₅₀ /MIC	
				dark	light	dark	light	dark	light
A	1	0	163.7	> 500	> 500	> 500	> 500		
AA	2	0	325.3	188	125	> 500	> 500	> 3	> 4
AAA	3	0	487.0	31	1.5	775	705	25	481
AAAA	4	0	506.2	31	2.0	584	415	19	212
AB	2	1/2	259.8	63	31	255	185	4	6
ABA	3	1/3	421.5	16	4.9	243	174	16	36
AAB	3	1/3	421.5	16	0.85	102	67	6	78
ABAB	4	1/2	517.6	4	0.49	38	44	10	91
BAAB	4	1/2	517.6	8	0.49	36	14	5	29
BBAA	4	1/2	517.6	4	0.41	23	23	6	57
AABA	4	1/4	583.1	4	0.046	74	60	19	1311
ABABAB	6	1/2	775.4	313	31	518	128	2	4
1:1:1 mix AB, ABAB, and ABABAB	4	1/2	$M_{\rm n} = 517.6$ $M_{\rm w} = 603.2$ D = 1.17	16	3	64	73	4	24

^{*} **n** is the total number of thiophene units in the oligomer.

 f_{methyl} is the fraction of 3-methyl thiophene units in the co-oligomers.

⁺ MIC is the Minimum Inhibitory Concentration against *E. coli* (ATCC 25922) in MH broth.

Antibacterial Activity. The minimum inhibitory concentration (MIC) is defined as the lowest concentration of thiophene oligomer that completely inhibits the growth of bacterial cells (~10⁶ CFU/mL) in MH broth after incubation for 18 hours at 37 °C. In this report, we further define MIC_{dark} and MIC_{light} as the observed MIC values for incubation in the dark versus incubation under the illumination of a common desktop reading lamp (3.55 W LED bulb, distance 5 cm, ~320 lumens). It is important to emphasize that a *lower* value of MIC conveys *more potent* antibacterial activity.

In the dark, these thiophene oligomers exert potent antibacterial activity against E. coli, which depends sensitively on the chain length and comonomer composition (Figure 3 and Table 1). Generally, the antibacterial activity of $(AB)_{n/2}$ is enhanced (MIC_{dark} decreases) as the number of thiophene units in the chain is increased from two to four (n = 2, 4). Upon further elongation to six thiophene units (n = 6), the antibacterial activity is abruptly lost due to poor solubility of the hexamers in aqueous solution (precipitation from the

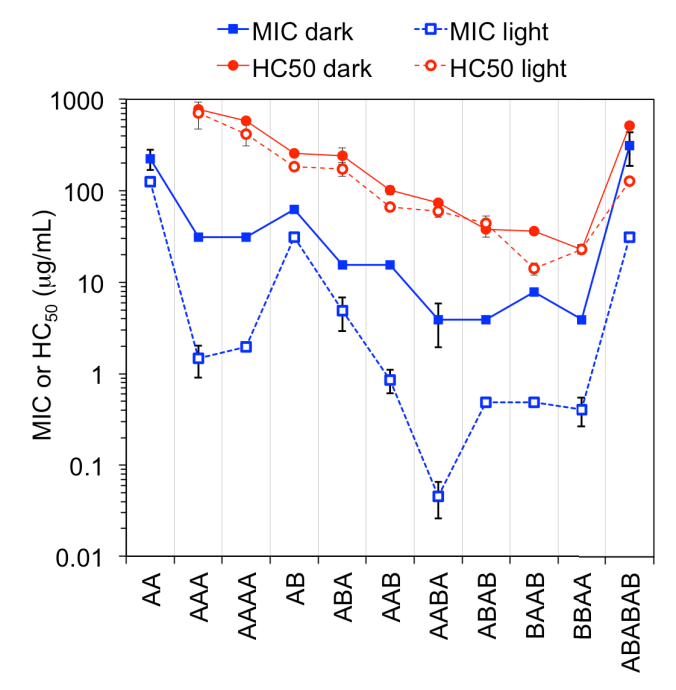


Figure 3. MIC and HC_{50} values of sequence-controlled, unimolecular oligothiophenes; both in the dark and under visible light. Thiophene tetramers exhibit remarkably potent antibacterial activity in the ng/mL range. The selectivity index, defined as SI = HC_{50} /MIC, is greatest in the case of **AABA** (SI > 1300). *E. coli* (ATCC 25922) was used in the MIC assays.

MH broth media is observed in the case of $[\mathbf{AB}]_3$). The comonomer composition also plays a prominent role in dictating the antibacterial activity. The amine-functionalized homo-oligomers of type $(\mathbf{A})_n$, where n = 1 to 4, are generally less active than the copolymers containing 50%

hydrophobic **B** units. The trimers with 33% hydrophobic groups (**ABA** and **AAB**) gave MIC values that are intermediate between those of the cationic homooligomers and the more hydrophobic tetramers **ABAB** and **BBAA**. Thus, we find that increasing the hydrophobicity enhances antibacterial activity (in the dark) up to a certain threshold near the solubility limit, beyond which activity is abruptly lost. These findings are well in accord with prior studies on HDP-mimetic copolymers. ⁵³

When exposed to visible light, the MIC values, for all trimers and tetramers in this library, decrease by orders of magnitude, which is the hallmark of a photodynamic antibacterial agent. For example, the MIC_{light} value of **ABAB** is 0.49 μ g/mL, which is much more potent than the same compound in the dark (MIC_{dark} = 4 μ g/mL). An exceptionally marked enhancement of activity

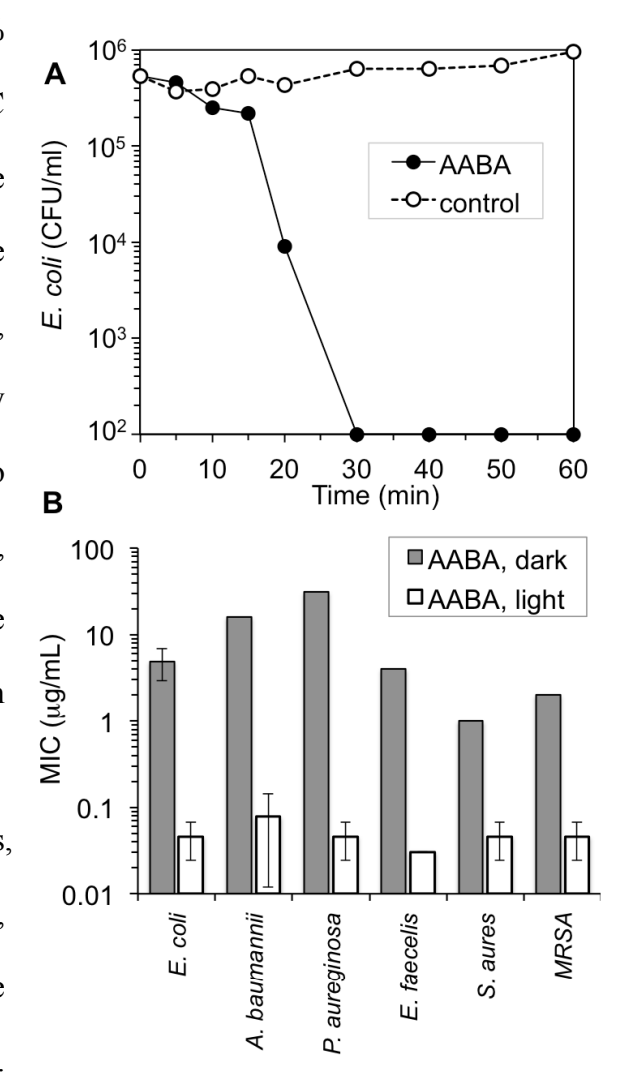


Figure 4. (A) Bactericidal kinetics of **AABA** against *E. coli* (ATCC 25922) under visible light illumination. (B) Broad spectrum antibacterial activity, in the light and dark, against a panel of Gram-positive and Gram-negative strains. The assays were performed three times in triplicate and error bars represent the standard deviation. In many cases, the same MIC was observed in each measurement and thus no error bars are visible.

was observed in the case of AABA, which gave $MIC_{light} = 0.046 \mu g/mL$ (46 ng/mL), an enhancement of 87-fold when compared to the activity of AABA in the dark (4 $\mu g/mL$). Thus, it is clear from the structure-activity data across this library of oligothiophenes that potent photodynamic antibacterial activity is sensitively dependent on the chain length, comonomer

composition, and sequence of the thiophene units in the oligomeric chain. This photodynamic enhancement of antibacterial activity is striking, especially when one considers that these relatively short oligomers of thiophene only absorb a fraction of the visible light spectra in the blue. Thus, further optimization of the amphiphilic balance among longer chains of thiophene (or other low bandgap backbone structures) is reasonably expected to yield even more potent and selective examples than those identified in this first-generation library screening. The monomer $\bf A$ and the dimers $\bf AA$ and $\bf AB$ do not absorb in the visible spectrum and thus are unaffected by illumination (MIC_{light} \sim MIC_{dark}), as expected.

Kinetics and Broad Spectrum. The compound **AABA** is a broad-spectrum antibacterial agent against a panel of Gram-positive and Gram-negative strains, including some notoriously problematic drug-resistant pathogens,⁵⁴ such as *A. baumanni* and methicillin-resistant *S. aureus* (MRSA). The MIC_{dark} values are all in the range of 1–32 μg/mL whereas MIC_{light} values are all below 100 ng/mL regardless of bacterial strain. The compound also exerts rapid bactericidal activity against *E. coli*. Under visible light, **AABA** induced a 4-log reduction (99.99% killing) in the number of viable *E. coli* CFU/mL, in just 30 minutes, at a concentration of just 100 *nano*grams/mL. Thus, we confirmed that **AABA** exerts extremely potent, broad-spectrum, and fast-acting photodynamic antibacterial agent (Figure 4). This compound is therefore a prime candidate for further study in terms of biological

Antibacterial Photomask. In order to visually highlight the spatial selectivity of photo-induced bactericidal action, we fabricated a simple photomask on the lid of a petri dish (diameter 6 cm) filled with MH

activity as well as mechanism of action.



Figure 5. Selective illumination of *E. coli* ($\sim 0.5 \times 10^6$ CFU/mL) and **AABA** (MIC_{dark} > 0.8 µg/mL > MIC_{light}) through a photomask enables spatial control of bacterial inactivation.

agar (Figure 5). A solution containing E. coli cells (10^6 CFU/mL) mixed with **AABA**, at a concentration above MIC_{light} but below MIC_{dark} ($0.8 \mu g/mL$), was spread onto the agar plate. The sample was then incubated for 18 hours, under visible light illumination. Colonies of E. coli grow preferentially in the regions where the mask casts a shadow on the agar surface whereas the growth is effectively suppressed in the regions that are illuminated (Figure 5). Thus, the notion that visible light selectively induces killing in this concentration range is clearly supported. This result is important because it illustrates how localized topical therapies could potentially be employed to solely attack the site of an infection without need for concern over side effects or toxicity in distant regions of space.

Hemolytic Activity. In order to assess the toxicity of the oligothiophenes compounds against mammalian cells, we employed a hemolysis assay with red blood cells (RBCs). The extent of cell lysis is monitored by quantifying the absorbance of hemoglobin released from the RBCs. The hemolytic concentration (HC₅₀) is defined as the concentration of the compound that induces 50% release of hemoglobin from the RBCs, relative to the positive control for complete lysis, TritonX-100. The hemolytic activity of these cationic, amphiphilic compounds is sensitively dependent on charge, hydrophobic content, and chain length. The cationic monomer **A** and the homodimer **AA** were both completely non-hemolytic up to the highest concentration tested (500 ug/mL). As the homooligomer chain length is further increased, weakly hemolytic behavior was observed for the trimer **AAA** (HC₅₀ = 775 μg/mL) and the tetramer **AAAA** (HC₅₀ = 584 μg/mL). For the amphiphilic oligomers bearing cationic and hydrophobic units in a 1:1 ratio, hemolytic activity also increases with chain length. The heterodimer **AB** is moderately hemolytic (HC₅₀ = 255 μg/mL), whereas the alternating tetramer **ABAB** is more potently hemolytic (HC₅₀ = 38

 $\mu g/mL$). On the other hand, the sparingly water-soluble **ABABAB** is only weakly hemolytic (HC₅₀ = 518 $\mu g/mL$), mainly due to precipitation from the assay media.

The effect of visible light illumination on the observed hemolytic activities was rather marginal, especially when compared to the remarkable enhancement of antibacterial activity under the same conditions. The HC_{50} values for nearly all compounds in the library are not substanially impacted by white light illumination ($HC_{50,light} \sim HC_{50,dark}$). For example, **AABA** is moderately hemolytic in the dark (74 µg/mL) and similarly in the light (60 µg/mL). We propose the simplest explanation for this remarkable observation is related to selective cell binding. We propose that the cationic oligomers preferentially bind to anionic components of the bacterial cell membranes, enabling localized production of toxic ROS near the target. In contrast, the relatively weak binding to RBC and HeLa membranes results in ROS production further away from the cells and thus has little effect. This idea is supported by the fact that ROS are generally very short-lived species in aqueous solution; thus, ROS production must occur within close range to a target in order to result in cell death.

From this initial screening, the most exceptional candidate, in terms of photodynamic potency combined with high cell type selectivity, is the tetramer **AABA** containing 25% hydrophobic side chains and bears a 3+ charge at neutral pH. The MIC_{light} value for this compound is a remarkable 46 ng/mL and the selectivity index (HC_{50,light}/MIC_{light} = 1311) is extremely high value a synthetic mimic of antimicrobial peptides.

Cytotoxicity. In addition to the hemoglobin-release assay using RBCs, we also quantified the cytotoxicity of these oligo(thiophene)s against HeLa cells using the CellTiter-Blue reagent from Promega, both in the light and dark conditions. This assay works by measuring the conversion of Resazurin to Resorufin, which occurs in a linear relationship dependent on the ability of viable

cells to reduce this molecule which can then be read in 96-well fluorescent plate reader at $\lambda_{Em} = 584$ nm. S5-56 Briefly, a confluent monolayer of HeLa cells was treated with media containing **AABA** at concentrations ranging from ~ 0.002 to $100 \,\mu\text{g/mL}$, incubated for 24 hours, and then evaluated to quantify the % cytotoxicity as a function of **AABA** concentration. The resulting dose-response curve is given in Figure 6.

In the dark, the compound showed an $LC_{50,dark}$ value of approximately 20 µg/mL (selectivity $LC_{50,dark}$ /MIC_{dark} = 434). The assay was repeated with a 30 min white light illumination of HeLa cells exposed to **AABA**, using the same exposure conditions as the antibacterial and hemolytic assays, followed by a 24 hr incubation in the dark. Under this condition, the $LC_{50, light}$ value (12 µg/mL) was only slightly lower than the

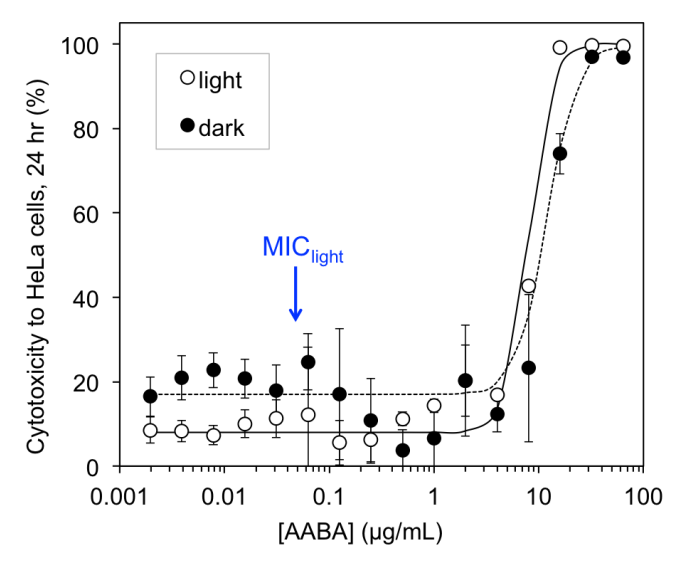


Figure 6. Dose response curve of the cytotoxicity of **AABA** to HeLa cells. Cells were exposed to indicated **AABA** concentration for a period of 24 hours. Cytotoxicity was measured using CellTiter-Blue assay. Toxicity is normalized to 3% CTAB (100% cytotoxic) and PBS (0% cytotoxic).

dark value, suggesting that the cytotoxicity against cultured mammalian cells is not as significantly impacted by ROS production, compared to the marked effects on bacterial cells (orders of magnitude enhancement of MIC under illumination).

Sequence Effects. Whereas each specific HDP is composed of a defined sequence of amino acids, ⁵⁷ there is no one conserved sequence across this very diverse class of peptides. ⁴⁸ Moreover, statistically random copolymers have been shown to exert HDP-mimetic activity despite their complete lack of sequence control. ^{9, 53, 58} But on the other hand, the *sequence distribution* of synthetic copolymers is known to play a major role in dictating the structure-activity

relationships; a direct comparison of block and random copolymers revealed marked differences in biological activity. ⁵⁹⁻⁶⁰ The Alabi group has beautifully demonstrated sequence effects in well-defined cationic oligo(thioetheramide)s. ⁶¹⁻⁶³ These studies encouraged us to consider the role of comonomer sequence in the context of photodynamic activity, which has never been studied to our knowledge.

Among the library of thiophenes in this work, it appears that the sequence of the comonomer units does impact the antibacterial and hemolytic activities, even when chain length and composition are held fixed. For example, the two oligomers **AAB** and **ABA** have exactly the same chain length and chemical composition, but differ only in the arrangement of cationic charges. The MIC_{dark} is the same for both (16 μ g/mL), but quite remarkably, their MIC_{light} values differ by a factor of \sim 6×. This result shows that sequence can play a subtle but important role, especially in terms of the photodynamic effect even if the activity in the dark is unaffected by sequence. On the other hand, the HC₅₀ values for **AAB** and **ABA** differ only by a factor of 2× in

both the dark and light. We speculate that the conformation of the thiophene oligomer in the membrane-bound state may depend on the sequence (Figure 7), in a manner analogous to "facially amphiphilic" secondary structures of HDPs at interfaces. The lowest energy conformation for regioregular P3HT features an alternating sequence of

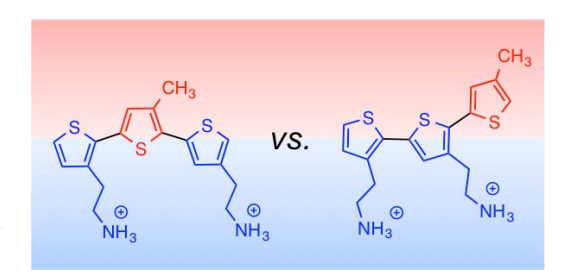


Figure 7. Putative conformations of **ABA** and **AAB** at a theoretical oil-water interface. Conformational changes related to sequence may impact their observed photodynamic activities, which differ by a factor of 6×.

conformers with every other side chain projected to opposite faces of the backbone.⁶⁴ In the present case, where every other unit bears a cationic charge, the structure is thus highly predisposed to adopt a "facially amphiphilic" conformation. Indeed, we designed the compounds

of type [AB]_n as alternating sequences based on the hypothesis that a facially amphiphilic lowest-energy conformer would promote localization at the water-membrane interface. But interestingly, ABA and AAB have the same MIC_{dark}, as do ABAB and BBAA, which implies that the membrane disruption mechanism is not highly sensitive to sequence at least at the trimer and tetramer level (in the dark). However, the significant difference (\sim 6×) in the MIC_{light} values for ABA and AAB would seem to suggest that ROS production (*vide infra*) within the membrane might be sensitive to sequence. This effect may be related to the conformation of the π -conjugated thiophene backbone, or its depth of penetration into the membrane, in the bound state. Schematically, one may envision the putative conformers of ABA and AAB localized at an oilwater interface as shown in Figure 6. Studies to examine the role of sequence in membrane binding and insertion, from both experimental and computational perspectives, are currently underway.

Dispersity Effects. Like HDPs, the oligo(thiophene)s in this study are discrete unimolecular molecules, as opposed to most synthetic antibacterial polymers, which inherently posses a statistical distribution of chain lengths and comonomer compositions. We sought to probe the role of dispersity in an exact manner, using these discrete thiophenes as model compounds. To that end, we prepared a mixture of **AB**, **ABAB** and **ABABAB** in a 1:1:1 *molar* ratio. The mixture is artificially disperse in terms of chain length (theoretically, D = 1.17), but has the exact same number average M_n (517.6) and composition (50% **A**) as the unimolecular tetramer **ABAB**. Hence, comparing the activity of **ABAB** to that of the mixture enables a simple and direct way to probe if dispersity plays any role. A similar strategy was employed recently to probe the effect of dispersity in unimolecular fractionated samples of P3HT.⁶⁵ The methods for calculation of $M_n = \sum_{i=1}^{n} M_i / \sum_{i=1}^{n} M_i / \sum_{i=1}^{n} M_i$, and $D = M_w / M_n$ are given in the SI document.

In the dark, the antibacterial potency of **ABAB** is 4-fold better than that of the mixture (MIC_{dark} = 4 versus 16 μ g/mL for the mixture) and the selectivity index is somewhat better as well (10× versus 4×). Under visible light, the effect is even more pronounced, with MIC_{light} = 3 μ g/mL for the artificially disperse mixture, compared to MIC_{light} = 0.5 μ g/mL for **ABAB** (a factor of 6×). Thus, it is evident that dispersity is indeed a significant determinant of biological activity. To our knowledge, no prior study has ever elucidated the role that dispersity plays in dictating the antibacterial and hemolytic activities, either for conventional antibacterial polymers or their photodynamic counterparts.

It is particularly informative to compare the MIC of the artificially disperse mixture to the theoretical *Reuss* average of MIC values (*activity* is inversely related to the effective *concentration*) for the components in the mixture **AB**, **ABAB**, and **ABABAB** as follows:

$$\frac{1}{\textit{MIC}_{mix}} \approx \frac{1}{\textit{MIC}_{Reuss}} = \frac{1/3}{\textit{MIC}_{AB}} + \frac{1/3}{\textit{MIC}_{ABAB}} + \frac{1/3}{\textit{MIC}_{ABABAB}}$$

which gives MIC_{Reuss} = 11 µg/mL and similarly HC_{50,Reuss} = 93 µg/mL. The experimental mixture is similarly antibacterial (MIC = 16 µg/mL) and hemolytic (HC₅₀ = 64 µg/mL) when compared to the predictions of the Reuss average, within less than a $2\times$ dilution in both cases. Considering these data, the activity of the blend appears to obey the expectation for a simple mixture but it deviates significantly from the unimolecular compound **ABAB** (Φ = 1). Hence, we show for the first time that *dispersity plays an important role* in dictating the biological activity of HDP-mimics, which has thus far received insufficient attention. It is also noteworthy that the dispersity studied here (Φ =1.17) would be considered very narrow in the context of synthetic polymer chemistry. Thus, truly unimolecular chain length does appear to confer an advantage relative to

even very highly controlled polymerization techniques, in terms of photodynamic antibacterial activity.

Induction of Resistance. One of the primary motivations for developing new antibacterial platforms is that bacteria readily develop resistance to conventional small molecule antibiotic

drugs. The membrane active HDPs and their synthetic mimics tend to be much less prone to induce resistance due to their physiochemically-driven membrane disrupting action. To our knowledge, induction of resistance is not widely explored in the field of photodynamic antibacterial polymers and oligomers. Thus, we sought to quantify the extent to which *E. coli* cells are able to

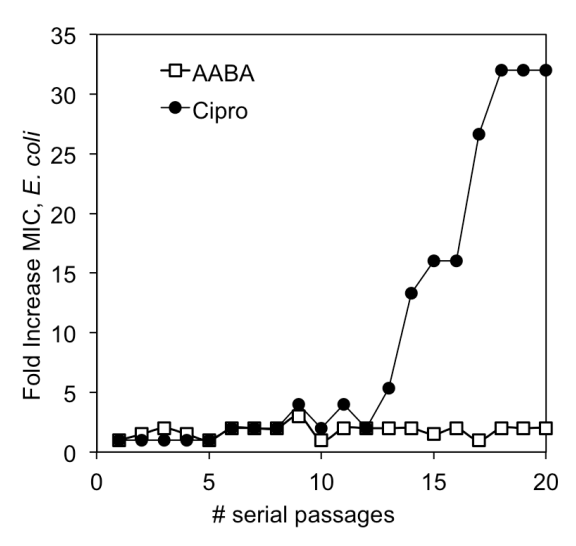
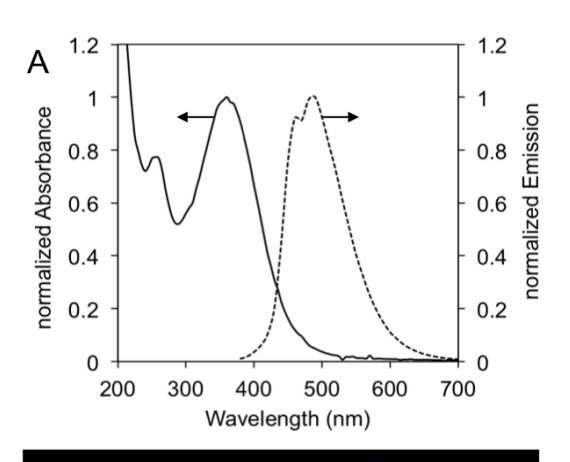


Figure 8. Induction of resistance by *E. coli* against Cipro and **AABA**.

develop resistance against the bactericidal effects of our lead compound in this study, **AABA**. Following the standard MIC test, cells are isolated from highest subinhibitory concentration of compound (½ MIC well), re-cultured in growth media, and re-subjected to the MIC test conditions. In the case where the MIC value remains largely unchanged as a function of serial sub-inihibitory passages, the compound does not induce resistance. In a direct comparison, we also evaluated the antibiotic drug Ciprofloxacin using the same method. Excitingly, our compound did not display any large change in the MIC value over the course of twenty subinhibitory passages, whereas the MIC of Cipro is increased (loss of potency) by a factor of 32× in the same conditions (Figure 8). Cipro had an initial MIC of 8 ng/mL but increased to 250 ng/mL after 21 subinhibitory passages. In contrast, **AABA** maintained a steady value of about 46

ng/mL across all passages. Hence, we can confidently conclude that **AABA** is much less prone to induction of resistance as compared to a standard antibiotic drug, in addition to outstanding potency and cell-type selectivity.

Bacteria Cell Imaging. The compound AABA exhibits an absorbance peak maximum at a wavelength of 380 nm and emits with a max near 515 nm in dilute aqueous solution. Since the compound itself is inherently emissive, we first examined the binding of **AABA** to *E. coli* cells with no other stains or dyes included. This enables a direct observation of the binding event without any possible changes to the system that may result from dye inclusion. Cells were treated with 0.8 µg/mL of **AABA**, which is above the MIC_{light} but below the MIC_{dark}, and then exposed to white light for 1 hour. Indeed, the confocal images showed a bright contrast in the blue, clearly revealing the smooth rod-shaped E. coli cells (Figure 9). That the E. coli maintains the characteristic shape suggests that the compound



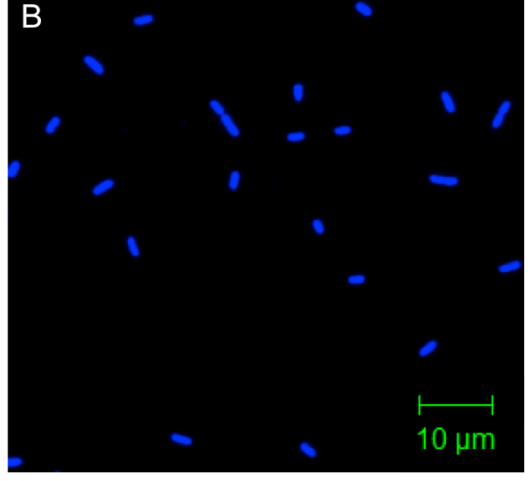


Figure 9. (A) Absorbance and emission spectra of **AABA** in aqueous buffer, (B) Confocal microscopy images of *E. coli* cells in PBS with **AABA** and no other dyes present.

binds to but does not completely lyse the cells, which effectively refutes the idea of a surfactant-like mechanism of action. It would appear that the emission intensity is uniformly distributed throughout the cells, which suggests uptake of the compound into the cytoplasm rather than accumulation solely on the membrane surface. This observation may suggest that the

polythiophenes penetrate cells by translocation of the membrane, perhaps even binding to intracellular targets. Such finer mechanistic details will be the subject of our ongoing investigations.

We next proceeded to examine the confocal images of the thiophene in combination with the commercially available LIVE/DEAD assay kit, which employs SYTO-9 and propidium iodide. The SYTO-9 (green channel) stains all cells, live or dead, whereas the PI (red channel) is a DNA-intercalation agent that cannot translocate healthy bacteria cell membrane. Thus, the PI only emits a signal when the membrane of the cell has been permeabilized. For this experiment, suspensions of *E. coli* were treated with **AABA** (0.8 μg/mL) and the mixtures were then stained with the LIVE/DEAD kit in media (Figure S2). The sample was exposed to visible light illumination for 1 hour. All cells showed bright red PI emission, indicative of cell death. All three signals (blue, red, and green) appear uniformly distributed throughout the rod-shaped cells. Thus, **AABA** kills bacteria cells at concentrations below MIC_{dark} but above MIC_{light}, leading to cellular uptake of the PI stain as well as the thiophene compound itself. The fact that the *E. coli* cells maintain their smooth rod-like morphology after cell death implies that the mechanism does

not depend on complete "surfactant-like" lysis of the cells. This result is potentially impactful because bacteriolytic antibiotics are known to induce endotoxin release and trigger sepsis. 66-68

ROS Production. We hypothesized that cationic and amphiphilic thiophene oligomers exert dual modes of action

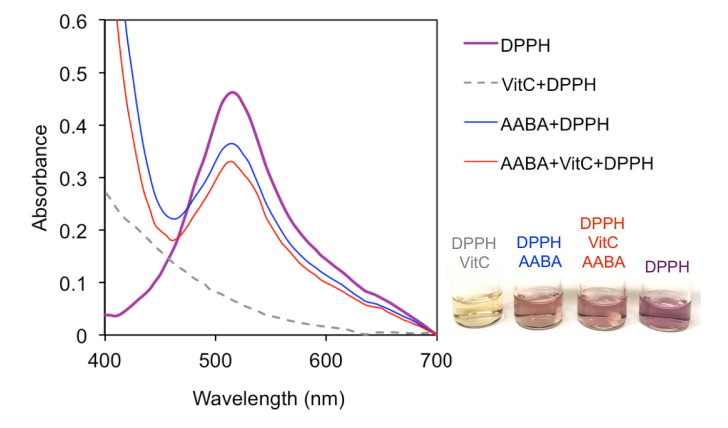


Figure 10. Oxidation of Vitamin C by **AABA** under visible light is evident in a DPPH colorimetric antioxidant activity assay.

involving both bacterial cell binding and ROS production. To probe the production of ROS by these thiophenes in solution, we employed an antioxidant activity assay using sodium ascorbate (Vitamin C) and the colorimetric probe 2,2-diphenyl-1-picrylhydrazyl (DPPH).⁶⁹ This probe is a stable free radical that absorbs visible light at 520 nm, but the absorbance intensity decreases upon reaction with antioxidants. For example, vitamin C reduces the DPPH and the solution color abruptly changes from a bright purple to pale yellow (Figure 10). The thiophene oligomer **AABA** was incubated with vitamin C (1:1 mol ratio) in aqueous solution under visible light illumination (1 hr, room temp), and then DPPH was added. No color change was observed and the absorbance peak at 520 nm persisted (Figure 10). ROS produced by thiophene in solution are expected to react with the sodium ascorbate and quench its antioxidant property. Indeed, the persistence of purple color of DPPH, in the presence of vitamin C/AABA mixtures, implies that the ROS produced by thiophene effectively abrogates the antioxidant activity of the vitamin compound (Figure 9). Thus, we confirm the notion that the bactericidal activity of these thiophene-based compounds is attributable to a photodynamic mechanism involving ROS production. Combined with the confocal images (Figures 9 and S2), we propose a putative mechanism of action that invokes selective bacterial binding (and/or cell penetration) combined with ROS production in the bound state, leading to selective inactivation of bacteria relative to mammalian red blood cells.

E. coli OM/IM Leakage. To quantify the membrane disruption process for the *E. coli* outer and inner membranes, an enzyme-chromogenic substrate assay was utilized. This approach exploits the periplasmic localization of the enzyme β-lactamase and the low permeability of the chromogenic substrate nitrocefin. Similarly, β-galactosidase is a cytoplasmic enzymer and the chromogenic substrate ortho-Nitrophenyl-β-galactoside (ONPG) exhibitis low cytoplasmic

membrane permeability. Only under conditions of membrane disruption can the substrates gain access to the corresponding enzyme, resulting in the production of a chromogenic product.⁷⁰

In the dark condition, **AABA** rapidly lyses the *E. coli* OM at concentrations ranging from 2 – 16 μ g/mL, which is similar to the MIC_{dark} value (Figure 11A). Interestingly, the OM permeabilization effect is similar in the case of visible light illumination (Figure 11C), suggesting that the production of ROS does not singificantly enhance or inhibit the membrane disruption process exerted by these oligomeric thiophene compounds. Moreover, the ONPG assay revealed that no substantial IM permeabilization was observed, in either the light or dark condition (Figure 11B and D), at concentrations as high as 64 μ g/mL. This result was surprising, because confocal images showed internalization of **AABA** into *E. coli* cells (not localization on the membrane) and the LIVE/DEAD stain assay confirmed PI uptake into cells. Moreover,

colony counting confirms that the bacterial cells are indeed dead, with >99.99% killing in this condition. It is difficult to rationalize these combined results with a pore formation model, since PI and the ONPG compound are similar in size: thus size-selective uptake of PI, but not ONPG, seems unlikely in the case of diffusion through discrete pores. Rather, we consider that **AABA** and PI are both rigid,

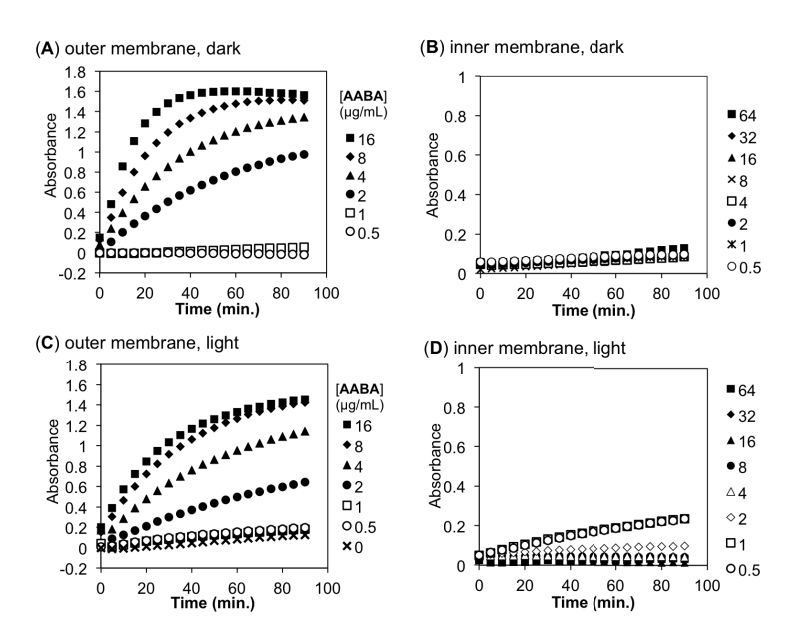


Figure 11. *E. coli* OM/IM leakage assay as a function of light exposure. (A, B) dark conditions, (C,D) light exposed conditions. (A,C) OM permeabilization assessed by nitrocefin conversion by β-lactamase, (B,D) IM permeabilization assessed by ONPG conversion by b-galactosidase. Positive controls for OM leakage using polymyxin B sulfate and for IM using CTAB are not shown. Data are averages of 3 independent replicates.

aromatic and cationic structures whereas the ONPG probe is hydrophilic and Zwitterionic. Perhaps for this reason, the cellular internalization of **AABA** (directly observed by confocal) may promote the co-translocation of PI across the polarized IM, even in the absence of discrete pore formation, whereas the hydrophilic ONPG would require water-filled channels in order to enter cells. More detailed mechanistic studies on the bactericidal action of these thiophene oligomers are currently underway in our laboratories.

Conclusions

Oligomers of thiophene bearing hydrophobic and cationic substituents in precisely defined sequence, with discrete unimolecular chain length and perfect regioregularity, effectively demonstrated the role of dispersity and sequence as determinants of antibacterial and hemolytic activities among photodynamic π -conjugated oligomers. To our knowledge, this is the first structure-activity relationship study on photodynamic mimics of host defense peptides (HDPs). By combining design principles from the HDP-mimicry field with the photodynamic therapy approach, we rapidly generated a library of oligo(thiophene) derivatives that display potent, rapid, broad-spectrum antibacterial activity when exposed to white light illumination. One of the key advantages in photodynamic therapy is the spatial control of bacterial inactivation, *i.e.* the bacterial lethality can be "turned on" exclusively at the site of infection, leaving other regions unaffected (and thus avoiding any systemic toxicity concerns). We demonstrated the *spatially selective* inactivation of bacterial colony growth on nutrient-rich agar by illumination through a photomask.

By comparison to the excellent antibacterial potency, the hemolytic activity against RBCs was orders of magnitude less potent; in one particularly striking example, the selectivity index HC_{50}/MIC was greater than 1300-fold, which is indicative of extremely high cell-type selectivity.

Cytotoxicity against HeLa cells demonstrated a similarly high level of cell-type selectivity. Moreover, bacteria cell binding was directly observed by confocal microscopy and ROS production was confirmed by a simple colorimetric assay. Permeabilization of *E. coli* outer membranes (OM) but not inner membranes (IM), both in the light and dark, was demonstrated by an enzymatic leakage assay. Finally, the compounds do not induce resistance upon 21 serial sub-inhibitory passages. Thus, we have identified a new molecular design platform for the optimization of photodynamic therapy using HDP-mimetic design principles. Further optimization and derivatization efforts among expanded libraries, as well as combined experimental and computational/simulation work to probe the mechanism of action, are currently underway in our laboratory and with others.

Experimental

General Synthetic Procedures. Detailed experimental procedures and all characterization data are given in the supporting information document. General protocols employed in the iterative convergent/divergent synthetic route are described herein.

OTBDMS protection. Imidazole (2.2 equiv) and tert-butyldimethyl silyl chloride (1.1 equiv) were dissolved in dry DMF and thiophene monomer or oligomer bearing hydroxyl side chains (1 equiv) was added in a single portion. The reaction was stirred at 35 °C overnight. The mixture was quenched with saturated aq. Sodium carbonate and extracted with EtOAc followed by washing with DI water and brine, drying over sodium sulfate. After filtration, solvent was removed *in vacuo*, the crude oil was purified by silica gel chromatography.

Bromination. At 0 °C, freshly recrystallized NBS (1 equiv) was added to a solution of thiophene monomer or oligomer (1 equiv) in dry THF under nitrogen atmosphere. The solution was stirred and allowed to warm to room temperature overnight. THF was removed under reduced pressure and mixture was dissolved in EtOAc, followed by washing with DI water and brine, and then drying over anhydrous sodium sulfate. After filtration and solvent evaporation, the crude oil was purified by silica gel chromatography

Stannylation. Lithium diisopropyl amide (LDA) was prepared by first dissolving diisopropyl amine (1 equiv) in hexane and THF (1:1) in an oven-dried Schlenk flask, cooling to -78 °C, and then injecting n-

BuLi (0.99 equiv). Then, the thiophene monomer or oligomer (1 equiv) in THF was added dropwise via cannula transfer. After 30 min, tributyltin chloride (1 equiv) was injected via syringe and the reaction mixture was stirred for 1 h at −78 °C. Upon warming to rt overnight, the reaction was quenched with saturated aq. sodium carbonate, and the crude reaction mixture was extracted with EtOAc, followed by washing with DI water and brine, drying over magnesium sulfate, and evaporation under reduced pressure. The product was used without purification.

Stille Coupling. In an oven-dried storage flask with a Teflon valve seal, brominated thiophene (1.1 equiv) and stannylated thiophene (1.0 equiv) were dissolved in anhydrous toluene and subjected to 3× freeze/pump/thaw/cycles. Pd(Ph₃P)₄ (0.01 equiv) as a slurry in toluene was added and subjected to another 3× freeze/pump/thaw/cycles. The reaction vessel was sealed under vacuum with a Teflon valve, and then heated to 95 °C for 24–72 h, or until the appearance of a black precipitate. The reaction mixture was cooled to rt, diluted with THF, and stirred with 1M NaOH aq for 1 hr. The organic layer was washed with water and brine, dried over sodium sulfate, filtered, and concentrated under reduced pressure. Purification by silica gel column chromatography.

OTBDMS deprotection. Tetreabutylammonium floride (1M in THF, 2 equiv) was added to a solution containing the protected thiophene (1 equiv) in THF and stirred at room temperature overnight. The mixture was purified by silica gel column chromatography (Hex:EtOAc = 4:1) to yield product.

Conversion to Azide. First, the hydroxyl groups were tosylated as follows; at 0 °C, p-Toluenesulfonyl chloride (1.2 equiv) and thiophene (1 equiv) were dissolved in dry DCM and pyridine (1 equiv) was added in a single portion. The solution was allowed to warm to room temperature overnight. The mixture was extracted with EtOAc, followed by washing with DI water and brine, drying over sodium sulfate. After filtration, solvent was removed under high vacuum, and the crude oil was purified by silica gel chromatography (Hex: EtOAc = 9:1) to give the tosylated product. Next, azides were introduced as follows; tosylated thiophene (1 equiv) and sodium azide (2 equiv) were dissolved in dry DMF and the solution was heated and stirred at 60 °C for 2 hours. The mixture was extracted with EtOAc, washed with DI water and brine, and dried over sodium sulfate. After filtration, solvent was removed under high vacuum to give the product. Typically, near-quantitative yields were achieved.

Azide Reduction. Amine-functionalized thiophene oligomers were prepared by reduction of the azide with lithium aluminum hydride (LAH), followed by protonation with HCl and precipitation of the ammonium salt product. Thiophene bearing azide (1 equiv) was dissolved in dry THF and LAH (1.5 equiv) was added in a single portion and stirred for 2 hours at rt. The mixture was extracted with EtOAc, followed by washing with DI water and brine, and drying over sodium sulfate. After filtration, solvent was removed under high vacuum. Then the crude oil was dissolved in THF and excess HCl dioxane

solution was added. The mixture was stirred 30 minutes and dried under high vaccum. The crude product was precipitated from diethyl ether to give the final product.

Antimicrobial Activity. The minimum inhibition concentration (MIC) was defined as the lowest concentration of compound that completely inhibits the growth of bacteria ($\sim 0.5 \times 10^6$ CFU/mL) in nutrient-rich MH broth media, upon overnight incubation at 37 °C. Oligothiophene solutions were prepared as 2-fold serial dilutions from a DMSO stock (5 mg/mL). A single colony of *E. coli* ATCC 25922 was inoculated in Muller-Hinton (MH) broth at 37 °C in a shaking incubator overnight. The turbid suspension was diluted to $OD_{600} = 0.1$, regrown for 90 min ($OD_{600} = 0.5 - 0.6$), and then diluted to $OD_{600} = 0.001$ in MH broth. The bacterial suspension (90 μ l) was mixed with each polymer concentration (10 μ l) in a sterile 96-well round-bottom polypropylene microplate. The microplate was incubated for 16 hours at 37 °C either in dark or light. All set of polymers were tested twice, each in duplicate, on different days. As a positive growth control, dilutions of DMSO with no compound were prepared and tested in the same manner with *E. coli*. As a negative growth control (for sterility), MH broth alone with no bacteria was also tested in triplicate.

Hemolytic Activity. Hemolytic activity of thiophenes was determined by hemoglobin release assay. First, 1 mL of 10% (v/v) sheep red blood cells was centrifuged at 1000 rpm for 5 min and washed with PBS, pH 7.4, and this procedure was repeated twice. The resulting stock was diluted 10-fold in PBS to provide 1% (v/v) RBC assay stock. In a sterile 96-well round-bottom polypropylene microplate, 90 μ l of 1% (v/v) RBC assay stock was mixed with 10 μ l of each of the oligothiophene serial dilution. As a negative control: PBS, as a positive control 0.1% (v/v): Triton X-100 were used. Microplate was wrapped with parafilm, secured in orbital shaker at 37 °C and incubated at 180 rpm for 60 min. The microplate was centrifuged at 1000 rpm for 10 min. In another sterile microplate, 10 μ l of supernatant was diluted in 90 μ l PBS. The absorbance at 415 nm was recorded using a microplate reader. Hemolysis was plotted as a function of polymer concentration and the HC₅₀ that is described as the polymer concentration causing 50% hemolysis relative to the positive control. This value was estimated by the fitting the experimental data to the function H = 1/(1+(HC₅₀/[P])ⁿ) where H is the hemolysis fraction (H = [OD₄₁₅(polymer)-OD₄₁₅(buffer)]/[OD₄₁₅(TritonX)-OD₄₁₅(buffer)]), P is the polymer concentration, n and HC₅₀ are the curve fitting parameters. All experiments were repeated twice, each in duplicate, on different days. The absorbance values from each trial were averaged and then the HC₅₀ was calculated.

Confocal Microscopy. A single colony of *E. coli* ATCC 25922 was inoculated in Muller-Hinton broth at 37 °C in shaking incubator overnight. The turbid suspension was diluted to $OD_{600} = 0.1$, regrown for 90 min to midlogarithmic phase ($OD_{600} = 0.5 - 0.6$) in MH broth. Resulting suspension was centrifuged at 2000 rpm for 3 min and the supernatant was carefully removed by pipetting. The pellet was

resuspended in PBS of pH 7.4. The bacterial suspension was diluted to $OD_{600} = 0.1 \ (\sim 5 \text{x} 10^7 \text{ cells/ml})$. **AABA** solution (4 µg/ml in 0.4% (v/v) DMSO-PBS) was added into 4 ml of bacterial suspension to provide the final concentration of polymer of 0.8 µg/ml (in a range between MIC_{dark} and MIC_{light}). The suspension was incubated with cells at 37 °C for 180 min under light. Later, suspension was pipetted to resuspend cells and 5 µl of suspension was placed on NuncTM glass bottom dish (Thermo Fisher Scientific) and covered with glass cover slip to be visualized under laser scanning confocal microscopy.

E. coli Outer Membrane (OM) Permeabilization Assay. Permeabilization of the *E. coli* OM was performed as described previously. A singular *E. coli* D31 colony was transferred into LB broth with 100μg/mL ampicillin (LB-Amp) followed by incubated at 37 °C with shaking for 18 hours. The inoculated culture was diluted into fresh LB-Amp at a 1:240 ratio. The diluted culture was placed back in incubation at 37 °C with shaking until OD₆₀₀ reached 0.2-0.6. Once the appropriate OD₆₀₀ was achieved, the culture was centrifuged at 2500 rpm for 15 minutes in a benchtop clinical centrifuge. Supernatant was discarded and the pellet resuspensed in identical volume of PBS. Nitrocefin solution was prepared dissolving 1mg nitrocefin in 100μL DMSO with subsequently dilution with 1.9mL PBS to achieve a final stock concentration of 500μg/mL. Nitrocefin solution was covered in aluminum foil and stored at 4 °C before dispensing into plates. Solutions were dispensed into a 96 well plate in the subsequent order: 10μL of oligo(thiophene)s with serial dilutions starting from 64μg/mL (excluding the last row containing 10μL distilled H₂O), 80μL E.coli, and 10μL of 500μg/mL nitrocefin. Following the addition of nitrocefin to the wells, the absorbance was immediately recorded at 486nm and was recorded every 5 minutes over the next 90 minutes.

E. coli Inner Membrane (IM) Permeabilization Assay. IM permeabilization was performed as described previously. The procedure follows that of the OM permeabilization assay, described above, with several modifications. A singular *E. coli* D31 colony was inoculated into 3mL of LB broth for 18 hours at 37 °C with shaking, followed by a 240-fold dilution into fresh LB broth supplemented with 100μL of 100mM Isopropyl β-D-1-thiogalactopyranoside (IPTG) to induce expression of the galactosidase gene. The diluted culture was incubated with shaking until an OD₆₀₀ of 0.2-0.5 was achieved. The following solutions were transferred into each well of a 96 well plate in the order listed: 56μL of Z-buffer, 10μL of serial diluted oligo(thiophene)s starting from 64μg/mL (except the last row containing 10μL distilled H2O), 19μL *E. coli* D31, and 15μL of 4mg/mL ortho-Nitrophenyl-β-galactoside (ONPG) in Z-buffer. Immediately after ONPG addition, absorbance was recorded at 420nm every 5 minutes for 90 minutes

Cytotoxicity Assay. Cytotoxicity of AABA was evaluated in HeLa cells as assayed by CellTiter-Blue reagent from Promega. In this assay, active cellular metabolism is measured by the enzymatic conversion of Resarzurin to Resorufin (florescent at 590nm). HeLa cells were seeded into a 96-well flat bottom cell

culture plate at 100,000 cells per well and grown for 24hrs in 180uL of DMEM 10% FBS, 1% Pen/Strep, 1% L-Glut. After 24 hrs, cells were exposed to various concentrations (20uL) of AABA beginning at 64 ug/mL final concentration and serially diluted in 0.01% Acetic acid 2-fold to ~2 ng/mL. As a positive control for cytotoxicity, CTAB reagent was used at both 3% (completely cytotoxic) and 0.1% (partially cytotoxic), PBS was used as a negative control. One 96 well plate was exposed to "light" for 30 min at 2 inches distance, a second plate was kept in the dark for the same 30 min "dark". Both plates were incubated in a standard CO_2 incubator 5% CO_2 37 °C for 24 hours. Following 24hrs of incubation with AABA, 20uL of CellTiter-Blue reagent was added directly to plate, mixed and incubated at 37°C for 3 hrs and analyzed on Synergy HT florescent plate reader, with $\lambda_{Ex} = 485$ nm, $\lambda_{Em} = 590$ nm.

Acknowledgements

The authors wish to thank Kathy Lin for assistance with MIC assay data collection. E.F.P. gratefully acknowledges support from a 3M Non-Tenured Faculty Award and a National Science Foundation CAREER Award (DMR BMAT #1653418). Z.Z. was supported, in part, by the Army Research Office STIR grant 66992-CH-II. C.E. was supported, in part, by a Presidential Graduate Research Fellowship from Rensselaer Polytechnic Institute. J.Y.L. and D.J.S. were supported by SURP fellowships from the College of Science and Mathematics at Rowan University.

Conflicts of Interest

The authors have no conflicts of interest to declare.

Supporting Information

Detailed materials and methods, synthetic procedures, NMR spectra, and additional experimental details. This information is available free of charge via the Internet at http://pubs.acs.org/.

References

- (1) Boucher, H. W.; Talbot, G. H.; Bradley, J. S.; Edwards, J. E.; Gilbert, D.; Rice, L. B.; Scheld, M.; Spellberg, B.; Bartlett, J. Bad Bugs, No Drugs: No ESKAPE! An Update from the Infectious Diseases Society of America. *Clin Infect Dis* **2009**, *48* (1), 1-12, DOI: 10.1086/595011.
- (2) Zasloff, M. Antimicrobial Peptides of Multicellular Organisms. *Nature* **2002**, *415* (6870), 389-395, DOI: 10.1038/415389a.
- (3) Jenssen, H.; Hamill, P.; Hancock, R. E. W. Peptide Antimicrobial Agents. *Clinical Microbiology Reviews* **2006**, *19* (3), 491-511, DOI: 10.1128/Cmr.00056-05.
- (4) Brown, K. L.; Hancock, R. E. W. Cationic Host Defense (Antimicrobial) Peptides. *Curr Opin Immunol* **2006**, *18* (1), 24-30, DOI: 10.1016/j.coi.2005.11.004.
- (5) Mishra, B.; Reiling, S.; Zarena, D.; Wang, G. S. Host Defense Antimicrobial Peptides as Antibiotics: Design and Application Strategies. *Curr Opin Chem Biol* **2017**, *38*, 87-96, DOI: 10.1016/j.cbpa.2017.03.014.
- (6) Tew, G. N.; Scott, R. W.; Klein, M. L.; Degrado, W. F. De Novo Design of Antimicrobial Polymers, Foldamers, and Small Molecules: From Discovery to Practical Applications. *Accounts Chem Res* **2010**, *43* (1), 30-39, DOI: 10.1021/ar900036b.
- (7) Mowery, B. P.; Lee, S. E.; Kissounko, D. A.; Epand, R. F.; Epand, R. M.; Weisblum, B.; Stahl, S. S.; Gellman, S. H. Mimicry of Antimicrobial Host-Defense Peptides by Random Copolymers. *J Am Chem Soc* **2007**, *129* (50), 15474-15476, DOI: 10.1021/ja077288d.
- (8) Ilker, M. F.; Nusslein, K.; Tew, G. N.; Coughlin, E. B. Tuning the Hemolytic and Antibacterial Activities of Amphiphilic Polynorbornene Derivatives. *J Am Chem Soc* **2004**, *126* (48), 15870-15875, DOI: 10.1021/ja045664d. (9) Kuroda, K.; DeGrado, W. F. Amphiphilic Polymethacrylate Derivatives as Antimicrobial Agents. *J Am Chem Soc* **2005**, *127* (12), 4128-4129, DOI: 10.1021/ja044205+.
- (10) Chin, W.; Zhong, G. S.; Pu, Q. Q.; Yang, C.; Lou, W. Y.; De Sessions, P. F.; Periaswamy, B.; Lee, A.; Liang, Z. C.; Ding, X.; Gao, S. J.; Chu, C. W.; Bianco, S.; Bao, C.; Tong, Y. W.; Fan, W. M.; Wu, M.; Hedrick, J. L.; Yang, Y. Y. A Macromolecular Approach to Eradicate Multidrug Resistant Bacterial Infections While Mitigating Drug Resistance Onset. *Nat Commun* **2018**, *9*, DOI: 10.1038/s41467-018-03325-6.
- (11) Matsuzaki, K. Control of Cell Selectivity of Antimicrobial Peptides. *BBA-Biomembranes* **2009**, *1788* (8), 1687-1692, DOI: 10.1016/j.bbamem.2008.09.013.
- (12) Brogden, K. A. Antimicrobial Peptides: Pore Formers or Metabolic Inhibitors in Bacteria? *Nat Rev Microbiol* **2005**, *3* (3), 238-250, DOI: 10.1038/Nrmicro1098.
- (13) Brogden, N. K.; Brogden, K. A. Will New Generations of Modified Antimicrobial Peptides Improve their Potential as Pharmaceuticals? *Int J Antimicrob Ag* **2011**, *38* (3), 217-225, DOI: 10.1016/J.Ijantimicag.2011.05.004. (14) Sahl, H. G. Biological Roles and Therapeutical Potential of Cationic Host Defence Peptides. *Biophys J* **2010**, *98* (3), 608a-608a.
- (15) Hancock, R. E. W.; Sahl, H. G. Antimicrobial and Host-Defense Peptides as New Anti-infective Therapeutic Strategies. *Nat Biotechnol* **2006**, *24* (12), 1551-1557, DOI: 10.1038/nbt1267.
- (16) Maisch, T.; Baier, J.; Franz, B.; Maier, M.; Landthaler, M.; Szeimies, R. M.; Baumler, W. The Role of Singlet Oxygen and Oxygen Concentration in Photodynamic Inactivation of Bacteria. *P Natl Acad Sci USA* **2007**, *104* (17), 7223-7228, DOI: 10.1073/pnas.0611328104.
- (17) Lu, L. D.; Rininsland, F. H.; Wittenburg, S. K.; Achyuthan, K. E.; McBranch, D. W.; Whitten, D. G. Biocidal Activity of a Light-absorbing Fluorescent Conjugated Polyelectrolyte. *Langmuir* **2005**, *21* (22), 10154-10159, DOI: 10.1021/la046987q.
- (18) Wang, Y.; Wang, H.; Guo, L.; Pang, Y.; Feng, L. Red Fluorescence Conjugated Polymer with Broad Spectrum Antimicrobial Activity for Treatment of Bacterial Infections In Vivo. *ACS Appl Mater Inter* **2018**, *10* (41), 34878-34885, DOI: 10.1021/acsami.8b10284.
- (19) Wang, Y.; Jett, S. D.; Crum, J.; Schanze, K. S.; Chi, E. Y.; Whitten, D. G. Understanding the Dark and Light-Enhanced Bactericidal Action of Cationic Conjugated Polyelectrolytes and Oligomers. *Langmuir* **2013**, *29* (2), 781-792, DOI: 10.1021/la3044889.
- (20) Chen, Z.; Yuan, H. X.; Liang, H. Y. Synthesis of Multifunctional Cationic Poly(p-phenylenevinylene) for Selectively Killing Bacteria and Lysosome-Specific Imaging. *ACS Appl Mater Inter* **2017**, *9* (11), 9260-9264, DOI: 10.1021/acsami.7b01609.
- (21) Yuan, H. X.; Liu, Z.; Liu, L. B.; Lv, F. T.; Wang, Y. L.; Wang, S. Cationic Conjugated Polymers for Discrimination of Microbial Pathogens. *Adv Mater* **2014**, *26* (25), 4333-4338, DOI: 10.1002/adma.201400636.

- (22) Ji, E. K.; Parthasarathy, A.; Corbitt, T. S.; Schanze, K. S.; Whitten, D. G. Antibacterial Activity of Conjugated Polyelectrolytes with Variable Chain Lengths. *Langmuir* **2011**, *27* (17), 10763-10769, DOI: 10.1021/la2018192.
- (23) Parthasarathy, A.; Pappas, H. C.; Hill, E. H.; Huang, Y.; Whitten, D. G.; Schanze, K. S. Conjugated Polyelectrolytes with Imidazolium Solubilizing Groups. Properties and Application to Photodynamic Inactivation of Bacteria. *ACS Appl Mater Inter* **2015**, *7* (51), 28027-28034, DOI: 10.1021/acsami.5b02771.
- (24) Zhu, C. L.; Yang, Q. O.; Liu, L. B.; Lv, F. T.; Li, S. Y.; Yang, G. Q.; Wang, S. Multifunctional Cationic Poly(p-phenylene vinylene) Polyelectrolytes for Selective Recognition, Imaging, and Killing of Bacteria Over Mammalian Cells. *Adv Mater* **2011**, *23* (41), 4805-4810, DOI: 10.1002/adma.201102850.
- (25) Yuan, H. X.; Wang, B.; Lv, F. T.; Liu, L. B.; Wang, S. Conjugated-Polymer-Based Energy-Transfer Systems for Antimicrobial and Anticancer Applications. *Adv Mater* **2014**, *26* (40), 6978-6982, DOI: 10.1002/adma.201400379.
- (26) Zhou, Z. J.; Corbitt, T. S.; Parthasarathy, A.; Tang, Y. L.; Ista, L. F.; Schanze, K. S.; Whitten, D. G. "End-Only" Functionalized Oligo(phenylene ethynylene)s: Synthesis, Photophysical and Biocidal Activity. *J Phys Chem Lett* **2010**, *1* (21), 3207-3212, DOI: 10.1021/jz101088k.
- (27) Zhao, Q.; Li, J. T.; Zhang, X. Q.; Li, Z. P.; Tang, Y. L. Cationic Oligo(thiophene ethynylene) with Broad-Spectrum and High Antibacterial Efficiency under White Light and Specific Biocidal Activity against S. aureus in Dark. *ACS Appl Mater Inter* **2016**, *8* (1), 1019-1024, DOI: 10.1021/acsami.5611264.
- (28) Wang, Y.; Jones, E. M.; Tang, Y. L.; Ji, E. K.; Lopez, G. P.; Chi, E. Y.; Schanze, K. S.; Whitten, D. G. Effect of Polymer Chain Length on Membrane Perturbation Activity of Cationic Phenylene Ethynylene Oligomers and Polymers. *Langmuir* **2011**, *27* (17), 10770-10775, DOI: 10.1021/la201820k.
- (29) Wang, B.; Wang, M.; Mikhailovsky, A.; Wang, S.; Bazan, G. C. A Membrane-Intercalating Conjugated Oligoelectrolyte with High-Efficiency Photodynamic Antimicrobial Activity. *Angew Chem Int Edit* **2017**, *56* (18), 5031-5034, DOI: 10.1002/anie.201701146.
- (30) Zhu, C. L.; Liu, L. B.; Yang, Q.; Lv, F. T.; Wang, S. Water-Soluble Conjugated Polymers for Imaging, Diagnosis, and Therapy. *Chem Rev* **2012**, *112* (8), 4687-4735, DOI: 10.1021/cr200263w.
- (31) Wang, J.; Zhuo, L. G.; Liao, W.; Yang, X.; Tang, Z. H.; Chen, Y.; Luo, S. Z.; Zhou, Z. J. Assessing the Biocidal Activity and Investigating the Mechanism of Oligo-p-phenylene-ethynylenes. *ACS Appl Mater Inter* **2017**, *9* (9), 7964-7971, DOI: 10.1021/acsami.6b16243.
- (32) Ergene, C.; Yasuhara, K.; Palermo, E. F. iomimetic Antimicrobial Polymers: Recent Advances in Molecular Design. *Polym Chem* **2018**, *9* (18), 2407-2427, DOI: 10.1039/c8py00012c.
- (33) Konai, M. M.; Bhattacharjee, B.; Ghosh, S.; Haldar, J. Recent Progress in Polymer Research to Tackle Infections and Antimicrobial Resistance. *Biomacromolecules* **2018**, *19* (6), 1888-1917, DOI: 10.1021/acs.biomac.8b00458.
- (34) Scott, R. W.; DeGrado, W. F.; Tew, G. N. De Novo Designed Synthetic Mimics of Antimicrobial Peptides. *Curr Opin Biotech* **2008**, *19* (6), 620-627, DOI: 10.1016/j.copbio.2008.10.013.
- (35) Takahashi, H.; Caputo, G. A.; Vemparala, S.; Kuroda, K. Synthetic Random Copolymers as a Molecular Platform To Mimic Host-Defense Antimicrobial Peptides. *Bioconjugate Chem* **2017**, *28* (5), 1340-1350, DOI: 10.1021/acs.bioconjchem.7b00114.
- (36) Som, A.; Vemparala, S.; Ivanov, I.; Tew, G. N. Synthetic Mimics of Antimicrobial Peptides. *Biopolymers* **2008**, *90* (2), 83-93, DOI: 10.1002/bip.20970.
- (37) Tew, G. N.; Liu, D. H.; Chen, B.; Doerksen, R. J.; Kaplan, J.; Carroll, P. J.; Klein, M. L.; DeGrado, W. F. De novo Design of Biomimetic Antimicrobial Polymers. *P Natl Acad Sci USA* **2002**, *99* (8), 5110-5114, DOI: 10.1073/pnas.082046199.
- (38) Choi, S.; Isaacs, A.; Clements, D.; Liu, D. H.; Kim, H.; Scott, R. W.; Winkler, J. D.; DeGrado, W. F. De novo Design and in vivo Activity of Conformationally Restrained Antimicrobial Arylamide Foldamers. *P Natl Acad Sci USA* **2009**, *106* (17), 6968-6973, DOI: 10.1073/pnas.0811818106.
- (39) Liu, D. H.; Choi, S.; Chen, B.; Doerksen, R. J.; Clements, D. J.; Winkler, J. D.; Klein, M. L.; DeGrado, W. F. Nontoxic Membrane-active Antimicrobial Arylamide Oligomers. *Angew Chem Int Edit* **2004**, *43* (9), 1158-1162, DOI: DOI 10.1002/anie.200352791.
- (40) Ding, L. P.; Chi, E. Y.; Schanze, K. S.; Lopez, G. P.; Whitten, D. G. Insight into the Mechanism of Antimicrobial Conjugated Polyelectrolytes: Lipid Headgroup Charge and Membrane Fluidity Effects. *Langmuir* **2010**, *26* (8), 5544-5550, DOI: 10.1021/la9038045.
- (41) Huang, Y.; Pappas, H. C.; Zhang, L. Q.; Wang, S. S.; Ca, R.; Tan, W. H.; Wang, S.; Whitten, D. G.; Schanze, K. S. Selective Imaging and Inactivation of Bacteria over Mammalian Cells by Imidazolium-Substituted Polythiophene. *Chem Mater* **2017**, *29* (15), 6389-6395, DOI: 10.1021/acs.chemmater.7b01796.

- (42) Chong, H.; Nie, C. Y.; Zhu, C. L.; Yang, Q.; Liu, L. B.; Lv, F. T.; Wang, S. Conjugated Polymer Nanoparticles for Light-Activated Anticancer and Antibacterial Activity with Imaging Capability. *Langmuir* **2012**, *28* (4), 2091-2098, DOI: 10.1021/la203832h.
- (43) Koch, F. P. V.; Smith, P.; Heeney, M. "Fibonacci's Route" to Regioregular Oligo(3-hexylthiophene)s. *J Am Chem Soc* **2013**, *135* (37), 13695-13698, DOI: 10.1021/ja4057932.
- (44) Zhou, Z.; Palermo, E. F. Templated Ring-Opening Metathesis (TROM) of Cyclic Olefins Tethered to Unimolecular Oligo(thiophene)s. *Macromolecules* **2018**, *51* (15), 6127–6137.
- (45) Gabriel, G. J.; Maegerlein, J. A.; Nelson, C. E.; Dabkowski, J. M.; Eren, T.; Nusslein, K.; Tew, G. N. Comparison of Facially Amphiphilic versus Segregated Monomers in the Design of Antibacterial Copolymers. *Chem-Eur J* **2009**, *15* (2), 433-439, DOI: Doi 10.1002/Chem.200801233.
- (46) Schmitt, M. A.; Weisblum, B.; Gellman, S. H. Interplay Among Folding, Sequence, and Lipophilicity in the Antibacterial and Hemolytic Activities of alpha/beta-Peptides. *J Am Chem Soc* **2007**, *129* (2), 417-428, DOI: 10.1021/ja0666553.
- (47) Mowery, B. P.; Lindner, A. H.; Weisblum, B.; Stahl, S. S.; Gellman, S. H. Structure-activity Relationships among Random Nylon-3 Copolymers That Mimic Antibacterial Host-Defense Peptides. *J Am Chem Soc* **2009**, *131* (28), 9735-9745, DOI: 10.1021/ja901613g.
- (48) Wang, Z.; Wang, G. S. APD: the Antimicrobial Peptide Database. *Nucleic Acids Res* **2004**, *32*, D590-D592, DOI: 10.1093/nar/gkh025.
- (49) Gelman, M. A.; Weisblum, B.; Lynn, D. M.; Gellman, S. H. Biocidal Activity of Polystyrenes that are Cationic by Virtue of Protonation. *Org Lett* **2004**, *6* (4), 557-560, DOI: 10.1021/ol036341+.
- (50) Palermo, E. F.; Kuroda, K. Chemical Structure of Cationic Groups in Amphiphilic Polymethacrylates Modulates the Antimicrobial and Hemolytic Activities. *Biomacromolecules* **2009**, *10* (6), 1416-1428, DOI: 10.1021/bm900044x.
- (51) Ergene, C.; Palermo, E. F. Cationic Poly(benzyl ether)s as Self-Immolative Antimicrobial Polymers. *Biomacromolecules* **2017**, *18* (10), 3400-3409, DOI: 10.1021/acs.biomac.7b01062.
- (52) Palermo, E. F.; Lee, D.-K.; Ramamoorthy, A.; Kuroda, K. Role of Cationic Group Structure in Membrane Binding and Disruption by Amphiphilic Copolymers. *J Phys Chem B* **2011**, *115* (2), 366-375, DOI: 10.1021/jp1083357.
- (53) Kuroda, K.; Caputo, G. A.; DeGrado, W. F. The Role of Hydrophobicity in the Antimicrobial and Hemolytic Activities of Polymethacrylate Derivatives. *Chem-Eur J* **2009**, *15* (5), 1123-1133, DOI: 10.1002/chem.200801523.
- (54) Rice, L. B. The Clinical Consequences of Antimicrobial Resistance. *Curr Opin Microbiol* **2009**, *12* (5), 476-481, DOI: 10.1016/j.mib.2009.08.001.
- (55) O'Brien, J.; Pognan, F. Investigation of the Alamar Blue (Resazurin) Fluorescent Dye for the Assessment of Mammalian Cell Cytotoxicity. *Toxicology* **2001**, *164* (1-3), 132-132.
- (56) O'Brien, J.; Wilson, I.; Orton, T.; Pognan, F. Investigation of the Alamar Blue (Resazurin) Fluorescent Dye for the Assessment of Mammalian Cell Cytotoxicity. *Eur J Biochem* **2000**, *267* (17), 5421-5426, DOI: 10.1046/j.1432-1327.2000.01606 x.
- (57) Hilpert, K.; Elliott, M. R.; Volkmer-Engert, R.; Henklein, P.; Donini, O.; Zhou, Q.; Winkler, D. F. H.; Hancock, R. E. W. Sequence Requirements and an Optimization Strategy for Short Antimicrobial Peptides. *Chemistry & Biology* **2006**, *13* (10), 1101-1107, DOI: 10.1016/j.chembiol.2006.08.014.
- (58) Schmitt, M. A.; Weisblum, B.; Gellman, S. H. Unexpected Relationships Between Structure and Function in alpha,beta-Peptides: Antimicrobial Foldamers with Heterogeneous Backbones. *J Am Chem Soc* **2004**, *126* (22), 6848-6849, DOI: 10.1021/ja048546z.
- (59) Oda, Y.; Kanaoka, S.; Sato, T.; Aoshima, S.; Kuroda, K. Block versus Random Amphiphilic Copolymers as Antibacterial Agents. *Biomacromolecules* **2011**, *12* (10), 3581-3591, DOI: Doi 10.1021/Bm200780r.
- (60) Kuroki, A.; Sangwan, P.; Qu, Y.; Peltier, R.; Sanchez-Cano, C.; Moat, J.; Dowson, C. G.; Williams, E. G. L.; Locock, K. E. S.; Hartlieb, M.; Perrier, S. Sequence Control as a Powerful Tool for Improving the Selectivity of Antimicrobial Polymers. *ACS Appl Mater Inter* **2017**, *9* (46), 40117–40126. DOI: 10.1021/acsami.7b14996
- (61) Porel, M.; Thornlow, D. N.; Artim, C. M.; Alabi, C. A. Sequence-Defined Backbone Modifications Regulate Antibacterial Activity of OligoTEAs. *ACS Chem Biol* **2017**, *12* (3), 715-723, DOI: 10.1021/acschembio.6b00837.
- (62) Porel, M.; Thornlow, D. N.; Phan, N. N.; Alabi, C. A. Sequence-Defined Bioactive Macrocycles via an Acid-catalysed Cascade Reaction. *Nature Chemistry* **2016**, *8* (6), 591-597, DOI: 10.1038/Nchem.2508.
- (63) Porel, M.; Alabi, C. A. Sequence-Defined Polymers via Orthogonal Allyl Acrylamide Building Blocks. *J Am Chem Soc* **2014**, *136* (38), 13162-13165, DOI: 10.1021/ja507262t.
- (64) Malik, S.; Nandi, A. K. Crystallization Mechanism of Regioregular Poly(3-Alkyl Thiophene)s. *J Polym Sci Pol Phys* **2002**, *40* (18), 2073-2085, DOI: 10.1002/polb.10272.

- (65) Lawrence, J.; Goto, E.; Ren, J. M.; McDearmon, B.; Kim, D. S.; Ochiai, Y.; Clark, P. G.; Laitar, D.; Higashihara, T.; Hawker, C. J. A Versatile and Efficient Strategy to Discrete Conjugated Oligomers. *J Am Chem Soc* **2017**, *139* (39), 13735-13739, DOI: 10.1021/jacs.7b05299.
- (66) Lepper, P. M.; Held, T. K.; Schneider, E. M.; Bolke, E.; Gerlach, H.; Trautmann, M. Clinical Implications of Antibiotic-induced Endotoxin Release in Septic Shock. *Intens Care Med* **2002**, *28* (7), 824-833, DOI: 10.1007/s00134-002-1330-6.
- (67) Holzheimer, R. G. Antibiotic Induced Endotoxin Release and Clinical Sepsis: a Review. *J Chemotherapy* **2001**, *13*, 159-172, DOI: 10.1179/joc.2001.13.Supplement-2.159.
- (68) Horn, D. L.; Opal, S. M.; Lomastro, E. Antibiotics, Cytokines, and Endotoxin: A Complex and Evolving Relationship in Gram-negative Sepsis. *Scand J Infect Dis* **1996**, 9-13.
- (69) Sharma, O. P.; Bhat, T. K. DPPH Antioxidant Assay Revisited. *Food Chem* **2009**, *113* (4), 1202-1205, DOI: 10.1016/j.foodchem.2008.08.008.
- (70) Shirley, D. J.; Chrom, C. L.; Richards, E. A.; Carone, B. R.; Caputo, G. A., Antimicrobial Activity of a Porphyrin Binding Peptide. *Peptide Sci* **2018**, *110* (4) e24074. DOI: 10.1002/bip.24074

Graphic for Manuscript:

